

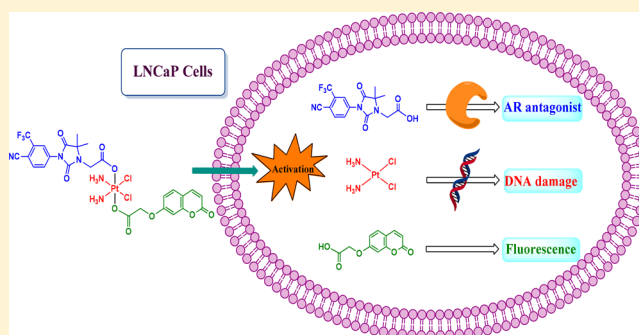
Theranostic Pt(IV) Conjugate with Target Selectivity for Androgen Receptor

Xiaodong Qin,^{†,‡,§} Lei Fang,^{†,‡,§} Jian Zhao,^{†,‡} and Shaohua Gou^{*,†,‡,§}

[†]Pharmaceutical Research Center and School of Chemistry and Chemical Engineering and [‡]Jiangsu Province Hi-Tech Key Laboratory for Biomedical Research, Southeast University, Nanjing 211189, China

Supporting Information

ABSTRACT: It is difficult to diagnose and treat castration-resistant prostate cancer (CRPC) which occurs due to the over-expression of androgen receptor (AR). Because there is a high level of AR in CRPC, we designed and prepared three Pt(IV)-based prodrugs targeting AR. Among them, compound 3, a three-in-one hybrid (an AR binding ligand, a cisplatin unit, and a coumarin moiety), was found to display satisfactory AR binding affinity and antagonist activity against androgen receptor, which could also be effectively internalized and visualized in LNCaP (AR+) cells. Due to its AR affinity, 3 selectively accumulated in greater quantities in LNCaP (AR+) cells than in PC-3 (AR-) cells. Moreover, compound 3 exhibited excellent anticancer activity superior to cisplatin. These results highlight the targeting theranostic application of Pt(IV) prodrugs.



INTRODUCTION

Prostate cancer (PC) is now one of the leading causes of cancer deaths in men worldwide.^{1,2} Depending on the diagnosis, treatment may involve surgical removal of the prostate gland or androgen depletion therapy (ADT). At present, nonsteroidal antiandrogens such as flutamide, bicalutamide, and nilutamide are the most commonly prescribed ADT drugs whose mechanism of action consists of competitively inhibiting androgen receptor (AR) activity associated with PC growth, division, and survival (Figure 1).^{3–5}

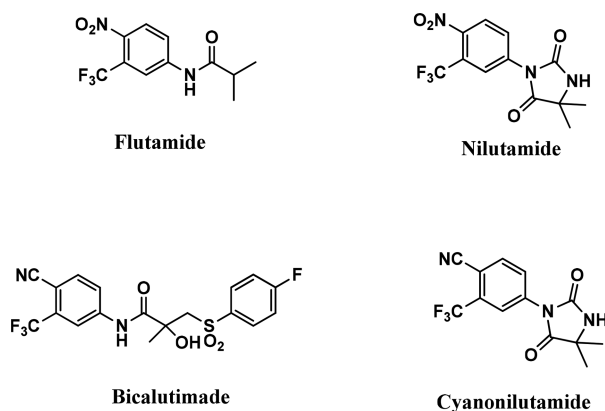


Figure 1. Examples of nonsteroidal antiandrogens reported in the literature.

Although these therapies are initially effective at suppressing tumor growth and improving survival, the tumor will eventually progress and develop into castration-resistant prostate cancer (CRPC),⁶ which is almost always incurable and often accompanied by poor

prognosis and metastatic spreading, with a median survival range from 18 to 24 months.⁷ Therefore, effective diagnosis and therapeutic treatments are needed to treat CRPC.

AR is a ligand-dependent transcription factor that is vital for the normal development and maintenance of the prostate. However, AR-mediated gene expression is also believed to act as an important driver throughout prostate cancer progression.^{8–10} Although the mechanisms responsible for the progression of PC to CRPC are not well-known, it has become clear that AR protein is essential for CRPC to adapt to the low levels of androgens.¹¹ It has been reported that the expression level of AR is approximately 6-fold higher in castration-resistant than hormone-sensitive prostate cancer.^{11,12} Hence, AR could be recognized as an attractive target for the treatment of CRPC.¹³ For example, Koch and co-workers have reported an androgen receptor-targeted nonsteroidal ligand for the tumor-specific delivery of a doxorubicin–formaldehyde conjugate.¹⁴ Oyelere et al. studied a series of hetero-bifunctional conjugates by conjugating nonsteroidal antiandrogen ligands with histone deacetylase inhibitors.¹⁵ Several promising agents including enzalutamide have been applied to improve CRPC patient survival;¹⁶ however, CRPC has evolved to be able to reactivate AR despite continued androgen depletion therapy.¹⁷ Therefore, discovery of more potent drugs beyond only acting on AR is needed.

Cisplatin (CDDP) is one of the most efficient drugs used for cancer chemotherapy. It binds to nuclear DNA, and then causes the blockage of replication and transcription, which ultimately leads to cellular apoptosis.^{18,19} However, the clinical efficiency

Received: January 10, 2018

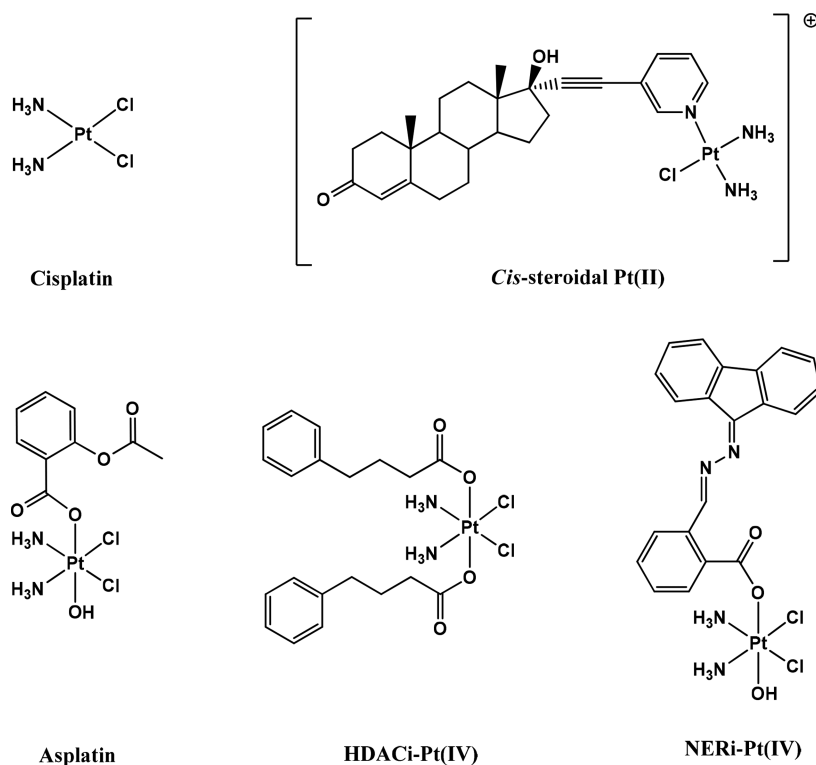


Figure 2. Chemical structures of cisplatin, *cis*-steroidal Pt(II), and several known Pt(IV) complexes.

of cisplatin is limited by several side effects such as nephrotoxicity, neurotoxicity, and ototoxicity mainly due to its nonspecificity.^{20,21} To overcome the nonspecificity of cisplatin, Rodger et al. developed a nonconventional Pt(II) complex that conjugates a steroidal androgen to target tumor cells (Figure 2).²² Over the past decade, the development of inert Pt(IV) prodrugs has been a promising strategy because the axial position of Pt(IV) complexes could be modified by various functional groups.^{23–25} On this basis, Lippard et al. reported a method to deliver cisplatin to prostate cancer cells by constructing Pt(IV)-encapsulated prostate-specific membrane antigen (PSMA), providing an avenue for systemic targeted therapy against this cancer.²⁶ Even though several Pt-based conjugates intended for prostate cancer treatment have been reported thus far,^{22,27} there are few reports to our knowledge describing the use of Pt-based complexes to conjugate a nonsteroidal unit targeting AR.

In order to introduce an AR-binding ligand to the axial position of Pt(IV) complexes and to develop selective and potent drugs to treat CRPC, here we report a few scaffolds composed of Pt(IV) complexes and nonsteroidal cyanonilutamide,^{14,15,28} which are expected to target PC via AR to endow the Pt(IV) prodrugs with favorable accumulation in cancer cells. In addition to assessing the cellular uptake and accumulation of Pt, a fluorescent agent (coumarin) was also introduced in a Pt(IV) prodrug to implement real-time imaging so that the cell uptake and targeting efficiency could be simultaneously visualized.

RESULTS AND DISCUSSION

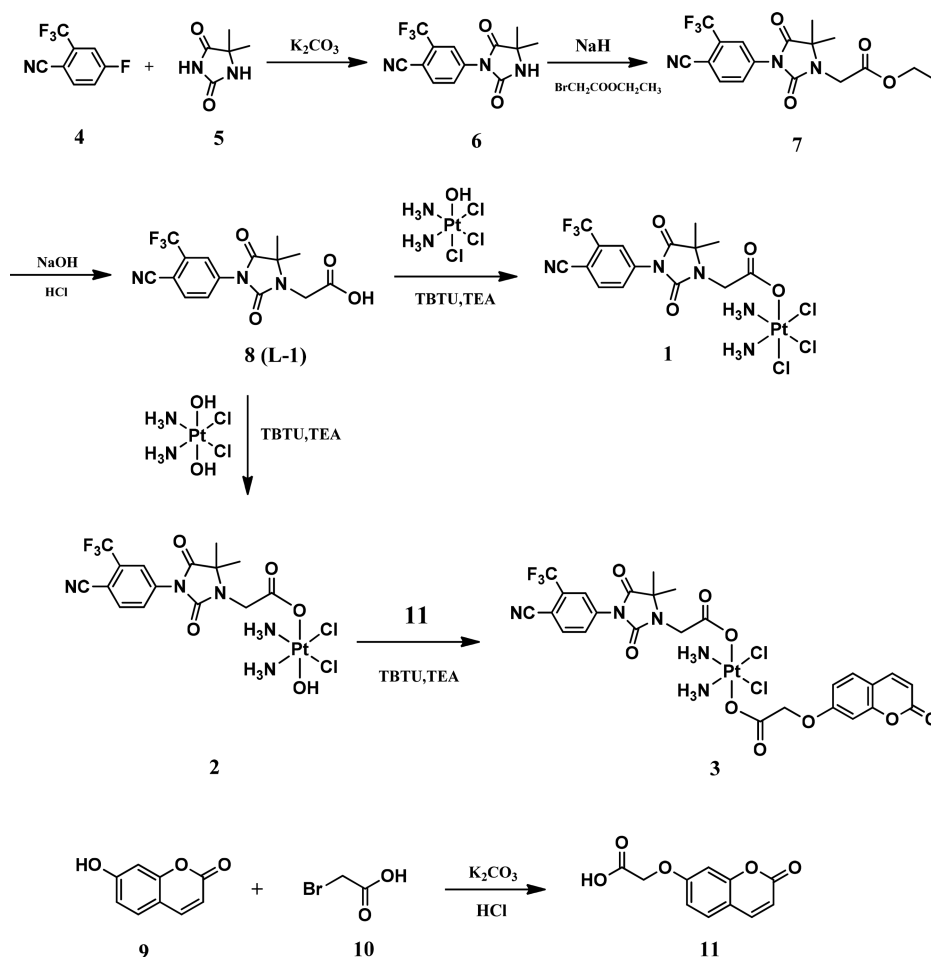
Design of an AR Ligand. To endow the Pt(IV) complex with AR-targeting ability, we designed a cyanonilutamide derivative (L-1) as the ligand (Scheme 1). Initial docking studies of L-1, cyanonilutamide and testosterone (an endogenous steroid that binds AR) were carried out to explore the binding capability in the cavity of helix-12 (H12, at the C-terminus of the

AR LBD).²⁹ The binding modes of these compounds were depicted in Figure 3 and the Surflex docking scores obtained were summarized in Table S1. The docking scores were 5.51 for L-1, 3.64 for cyanonilutamide, and 8.15 for testosterone, where higher scores indicated greater binding affinity. Although weaker than testosterone, the binding affinity of L-1 was greater than its parent compound cyanonilutamide. In Figure 3C, testosterone in complex with AR LBD showed that the carbonyl group had a hydrogen bond interaction with ARG752 and the hydroxyl group had a hydrogen bond with ASN705, contributing to the closed conformation of AR.³⁰ L-1, possessing a similar binding mode to cyanonilutamide, could also fit into the binding site by the formation of the key hydrogen bond between the cyano group and ARG752 (Figure 3A,B). The docking results suggested that L-1 had a competitive mechanism of action at the same site as testosterone, which might disturb the proper positioning of H12 and repress the activation of AR.

Synthesis. Three novel Pt(IV) prodrugs conjugated with L-1 were designed and synthesized (Scheme 1). Cyanonilutamide (6) was prepared according to the former literature report.²⁸ Compound 7 was synthesized via an alkylation of 6 with ethyl bromoacetate in the presence of sodium hydride. Then L-1 was obtained by the hydrolysis of 7. To explore the effect of ligands on the activity, complexes 1 and 2 were axially coordinated with chloridion and hydroxyl, respectively. Besides, a coumarin derivative (11) was introduced to the axial position of 2 to obtain a theranostic prodrug 3. All new compounds were unambiguously characterized by NMR spectroscopy and ESI-MS. The purity of Pt(IV) complexes 1–3 were confirmed to be more than 95% by HPLC.

Cyclic Voltammetry. To show how easily these compounds can be reduced to its Pt(II) equivalents, we measured the reduction potentials of complexes 1–3. In cyclic voltammograms (Figure S1, see Supporting Information), all complexes exhibited

Scheme 1. Synthesis of Pt(IV) Conjugates



irreversible reduction processes with the reduction potentials of 1–3 being -0.435 , -0.455 , and -0.467 V, respectively. The result indicated that the complex with an axial chlorido ligand (1) possessed the lowest electrochemical reducibility and the complex with an axial carboxylate ligand (3) possessed the highest electrochemical reducibility.

HPLC Analyses on the Stability and Reduction of Complexes 1–3. The solution stability and the reduction of complexes were examined by HPLC at different times. As shown in Figures 4A and S18–S20, all Pt(IV) complexes were stable in medium RPMI-1640 (10% fetal bovine serum) and PBS after 24 h. To further confirm whether the complex could be reduced to release its Pt(II) equivalent with the AR-targeting ligand and compare the reducing rate in the presence of ascorbic acid, each compound was investigated by HPLC in a mixture solvent of acetonitrile/water containing ascorbic acid. As seen in Figure S19, the absorption peak of 1 decreased upon reacting with VC and the peak of the AR-targeting ligand increased simultaneously as the time passed ($T_{1/2}$: 2.3 h, Figure 4). The similar phenomenon was observed when 2 was incubated with VC apart from the slower reducing rate ($T_{1/2}$: 8.8 h). As for 3, the reduction could also be observed with the longest time ($T_{1/2}$: 13.9 h), as shown by the presence of the AR-targeting ligand and coumarin moiety. Under the same condition, the experimental data of complexes 1–3 were all fitted well to a monoexponential decay function as described by previous reports.^{31–33} The rate constants (k_{obs}) of 1–3 were 0.3010 h^{-1} , 0.0792 h^{-1} , and 0.0501 h^{-1} , respectively. The chemical reduction rate of 2 was

slower than 1, indicating that an axial chlorido ligand in the coordination sphere would facilitate the electron transfer better than an axial hydroxyl ligand. In contrast, 3 displayed the slowest chemical reduction rate, demonstrating that carboxylates do not facilitate the electron transfer from the reducing agent to the Pt(IV) center.³⁴ However, no peak of the supposed cisplatin species was observed in HPLC chromatograms under the test condition, which was due to its weak chromophore in the UV detecting condition. It was noted that the reducing rate trend of complexes monitored by HPLC was in accordance with that measured by cyclic voltammetry. These observations revealed that the Pt(IV) complexes were stable in PBS and could be reduced to release the axial ligand(s) in the presence of ascorbic acid.

AR Binding Affinity. In order to explore the AR binding affinity of the new cyanonilutamide derivatives, the fluorescence polarization (FP) based binding assay by competition with the fluorescent tracer was carried out. As shown in Table 1, such derivatives retained the ability to bind AR directly, while cisplatin had no apparent binding affinity. The values of AR affinity for cyanonilutamide and bicalutamide were 4.42 and $2.51 \mu\text{M}$, respectively, a little different from those in the previous report.¹⁵ Considering that the values were in the same order, our results were convincing as well. L-1 showed the highest binding affinity with an IC_{50} value of $3.75 \mu\text{M}$ among the new cyanonilutamide derivatives. Meanwhile, 1–3 displayed a little weaker binding affinities with IC_{50} values in the range from 5.49 to $7.58 \mu\text{M}$. The tiny decline might be owing to the bigger size of the Pt(IV)

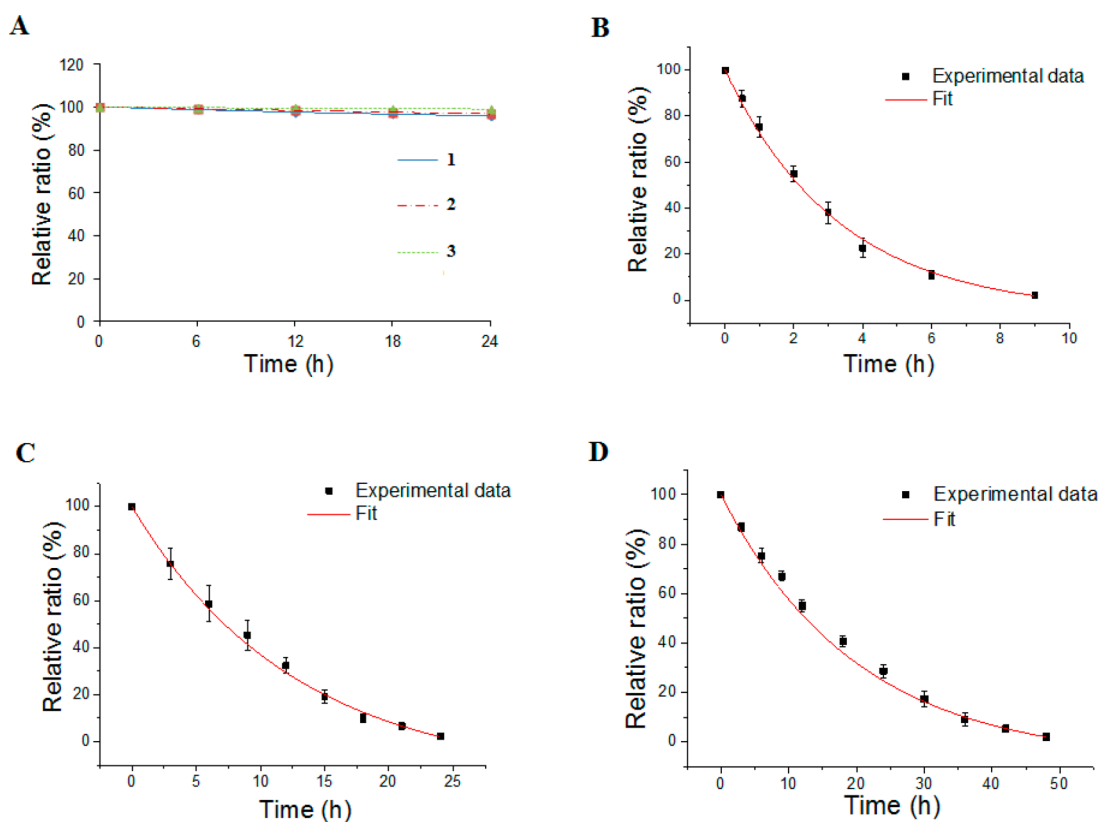


Figure 4. (A) Stability of 1–3 in medium RPMI-1640 (10% fetal bovine serum). Time-dependent reductions of 1 (B), 2 (C), and 3 (D) upon VC on HPLC (1–3 were 0.2 mM and VC was 1 mM). The experimental data of complexes 1–3 were fitted well to a monoexponential decay function (equation: $y = y_0 + A_1 \exp(-x/t_1)$, $k_{\text{obs}} = \ln(2)/t_1$).

Table 1. AR Binding Affinity and AR Antagonist Activity of Bicalutamide, Cyanonilutamide, Testosterone, Cisplatin, L-1, and complexes 1–3

compound	IC ₅₀ (μM)	inhibition % ^a (10 μM)
bicalutamide	2.51 ± 0.06	85.4
cyanonilutamide	4.42 ± 0.12	77.8
L-1	3.75 ± 0.10	51.2
1	5.49 ± 0.14	73.5
2	6.13 ± 0.10	66.3
3	7.58 ± 0.19	70.1
testosterone	0.0095 ± 0.0006	NT ^b
cisplatin	ND ^c	ND

^aInhibition rate was shown as a ratio to the R1881 control and the data represent the mean of at least three independent experiments.

^bNT, not tested. ^cND, not determined.

fluorescence under the same treatment with **11** (the precursor of **3**). As the stronger fluorescence often means higher cellular uptake, we could deem that the uptake of **3** was more than that of **11** in LNCaP cells. The results proved that the AR targeted ligand could significantly increase the uptake of **3** in AR over-expressed LNCaP cells and the conjugate could meet the requirement for cell imaging.

Cellular Uptake. Since the cytotoxic effect of Pt-based anti-cancer drugs is highly dependent on cellular uptake and accumulation, we explored the effect of the AR-ligand conjugation on the accumulation of the Pt(IV) complexes. For this purpose, the cellular uptake of the Pt(IV) complexes was determined by inductively coupled plasma mass spectrometry (ICP-MS) in both AR-positive LNCaP and AR-negative PC-3 cells. As shown in Figure 7,

the uptake of three Pt(IV) complexes did not exhibit apparent improvement compared with that of cisplatin in PC-3 (AR−) cells. However, in LNCaP (AR+) cells, complexes 1–3 accumulated in a higher extent than cisplatin. This suggested that the conjugation of the AR ligand with Pt(IV) units resulted in the increased cellular uptake, which might account for their higher cytotoxicity in AR-positive LNCaP cells. Moreover, complexes 1–3 preferentially accumulated in LNCaP (AR+) cells compared with PC-3 (AR−) cells, but in contrast, there was almost no difference in the control group of cisplatin. The amount of the platinum uptake of complex **3** was in accordance with the result in cell imaging experiments. These data clearly demonstrated that AR-targeted conjugates displayed the greater abilities of accumulation and selectivity owing to the acquired AR binding affinity.

In Vitro Cytotoxicity. To investigate cell-type selectivity and potency, we estimated the antiproliferative activity of these compounds in LNCaP (AR+) and PC-3 (AR−) cells. The in vitro cytotoxicity of the novel compounds against the two cell lines was evaluated by the MTT assay with cisplatin, bicalutamide and cyanonilutamide as reference controls. The corresponding IC₅₀ values (concentration required to reduce viability to 50%) obtained after 72 h exposure were summarized in Table 2. Bicalutamide showed moderate antiproliferative activity in LNCaP cells and no apparent activity in PC-3 cells, whereas cyanonilutamide had no activity in both cells. Not surprisingly, the IC₅₀ value of cisplatin in LNCaP cells was higher than that in PC-3 cells (SI = 0.75), which was consistent with the previous report.²⁶ This result indicated that cisplatin did not show any pronounced AR dependency in its cytotoxicity to either cell lines. However, it was gratifying to observe that all three complexes are

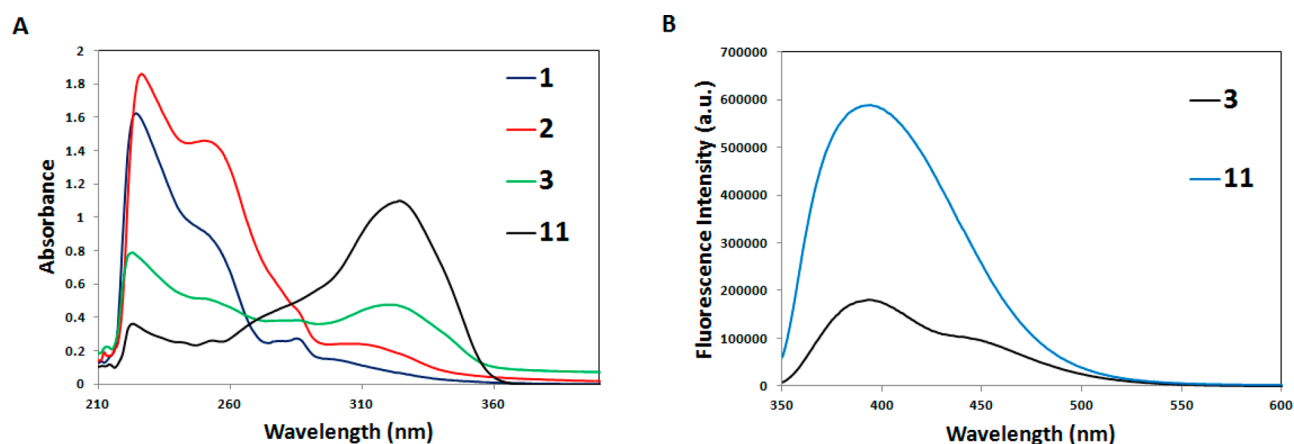


Figure 5. (A) Absorption of complexes 1–3 and 11. (B) Fluorescence spectra of 3 and 11. Compounds were dissolved in PBS containing 5% DMF at the concentration of 0.1 mM.

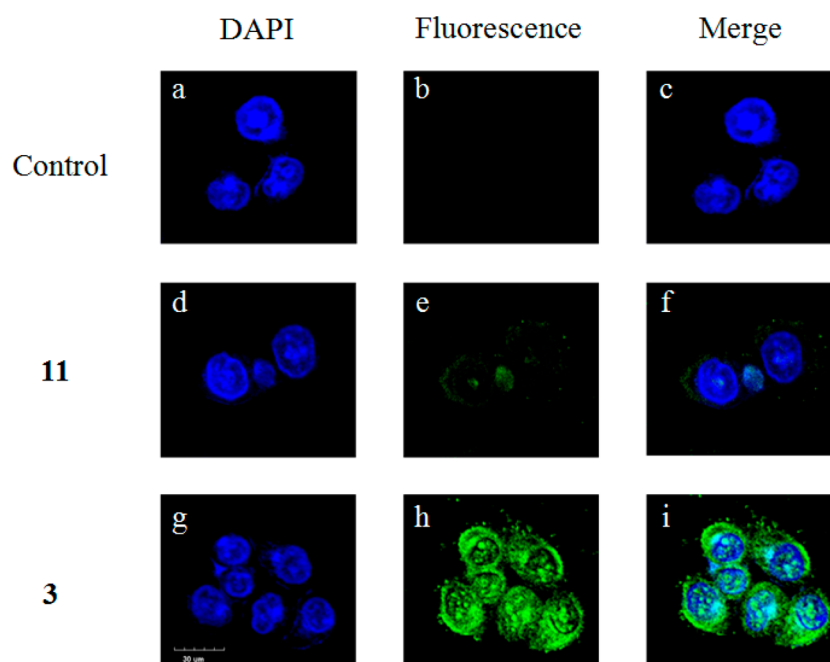


Figure 6. Confocal microscopy images of LNCaP cells treated with 20 μM compound 11 (d–f), 20 μM prodrug 3 (g–i), or untreated control cells (a–c). Fluorescence from DAPI staining nucleus appears as blue signals (Ex: 340 nm; Em: 450–470 nm) in the left column while fluorescence from 11 or 3 appears as green signals (Ex: 355 nm; Em: 490–520 nm) in the middle column. The right column was the merge of both above. Scale bar: 30 μm .

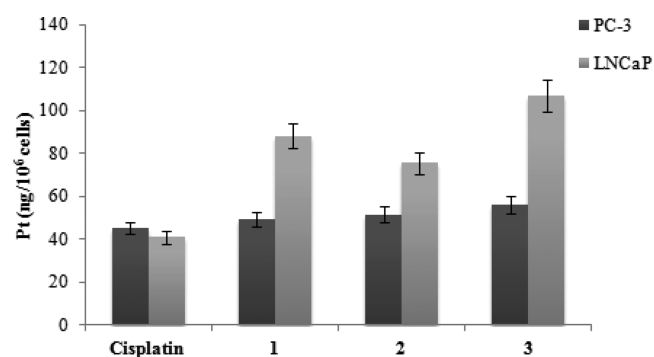


Figure 7. Cellular uptake of cisplatin and 1–3 in PC-3 and LNCaP cells after 12 h of incubation.

generally more cytotoxic against AR-dependent LNCaP cells than them against AR-independent PC-3 cells. More significantly,

Table 2. In Vitro Cytotoxicity of Cisplatin, Bicalutamide, Cyanonilutamide, L-1, 11, and Complexes 1–3

compound	IC ₅₀ (μM)		SI ^a
	PC-3 (–)	LNCaP (+)	
cisplatin	7.31 \pm 0.29	9.78 \pm 0.48	0.75
bicalutamide	>50	47.39 \pm 1.85	
cyanonilutamide	>50	>50	
L-1	>50	>50	
11	>50	>50	
1	6.88 \pm 0.51	3.15 \pm 0.27	2.18
2	5.79 \pm 0.39	2.87 \pm 0.15	2.01
3	2.84 \pm 0.25	1.02 \pm 0.08	2.78

^aSI (Selectivity Index) is defined as IC₅₀ value in PC-3 cells/IC₅₀ value in LNCaP cells.

all Pt(IV) complexes displayed enhanced activity superior to cisplatin. The results demonstrated that the ability of these

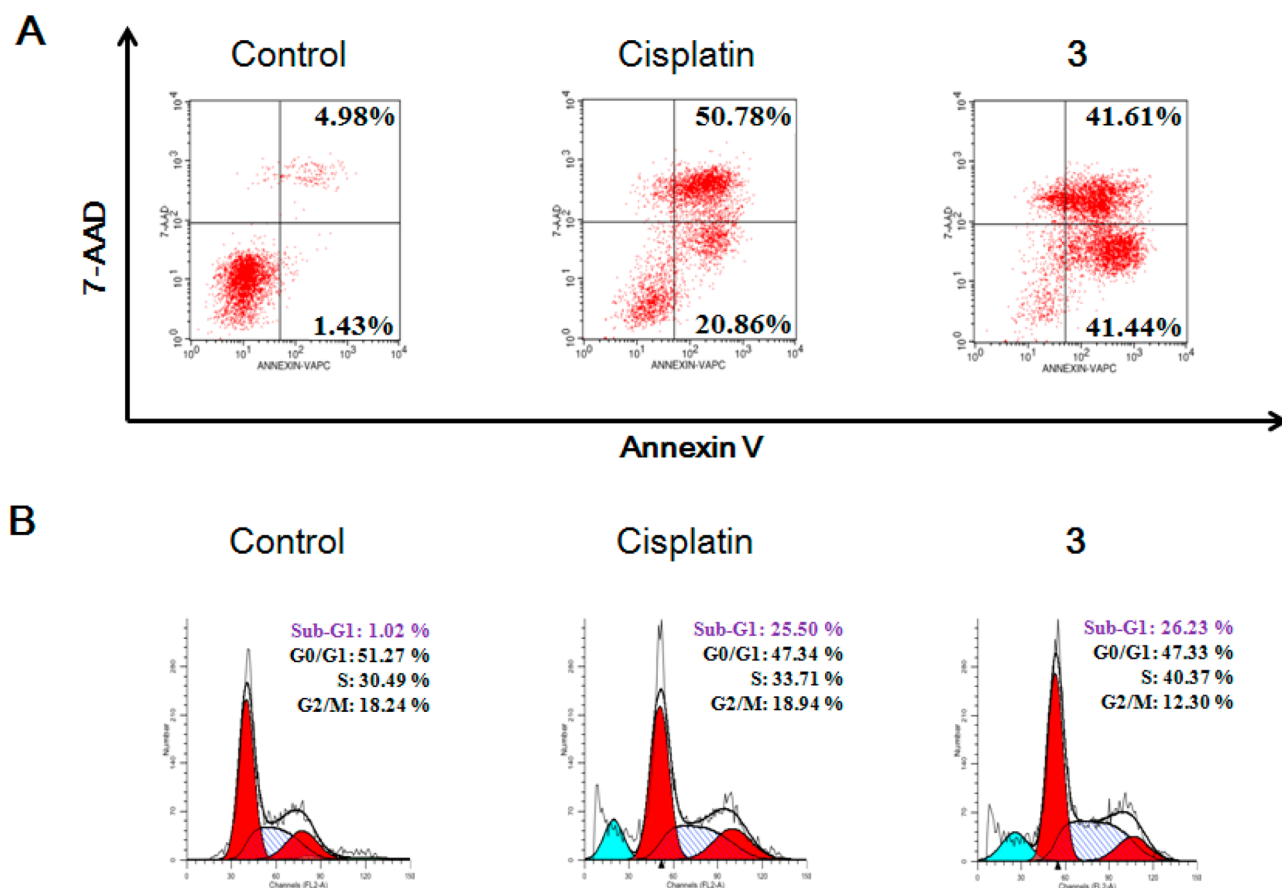


Figure 8. Flow cytometry analysis for apoptosis (A) and cell cycle distribution (B) of LNCaP cells induced by cisplatin or 3 at 20 μM for 24 h.

AR-Pt(IV) conjugates to bind to AR has indeed conferred cell-type selectivity and improved the antitumor effect remarkably. Notably, the theranostic prodrug 3, conjugated with a AR-targeting ligand and the coumarin moiety simultaneously, was 9.6 \times more active than cisplatin and exhibited the best selectivity (SI = 2.78).

Cell Cycle and Apoptosis Analysis. Since prodrug 3 displayed the best antitumor activity in vitro, we chose 3 as the optimal candidate for further therapeutic mechanism investigation. To evaluate whether the inhibition of the cancer cell proliferation was associated with apoptosis, an Annexin V-FITC/PI staining assay was carried out in LNCaP cells. The flow cytometry analysis showed that cisplatin achieved an apoptosis rate of 71.6% (including the early and late apoptosis). In contrast, 3 could achieve an apoptosis rate of 83.0%, much superior to that of cisplatin apparently (Figure 8A). Additionally, we also assessed the effect of 3 on cell cycle by measuring DNA content. LNCaP cells were still treated with 20 μM cisplatin and 3 for 24 h, and then cell cycle distribution was tested. As shown in Figure 8B, the percentage of sub-G1 phase, which is considered as a biomarker for DNA damage and related to the presence of apoptosis, increased apparently when treated with cisplatin or 3. Moreover, the cell cycle slightly changed after incubation with cisplatin: the percentage of G0/G1 phase decreased from 51.27% to 47.34%, the percentage of S phase increased from 30.49% to 33.71%, while the percentage of G2/M phase showed no obvious variations, respectively. However, the LNCaP cells were significantly arrested at S phase (40.37%) after incubation with 3, revealing that 3 possessed the stronger cell cycle arrest than cisplatin.

Western Blot Analysis. To gain more insights into the molecular mechanisms the activity of complex 3, we measured

the level of proteins related to the regulation of apoptosis by Western blotting. In Figure 9, the combined treatment with

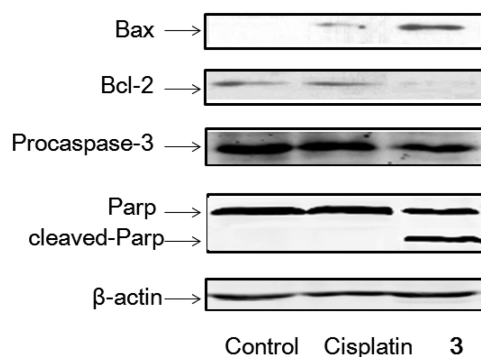


Figure 9. Western blotting analysis of the expression of related proteins.

cisplatin increased the expression of pro-apoptotic gene Bax and suppressed the expression of antiapoptotic gene Bcl-2. Excitingly, 3 showed a stronger effect on Bax and Bcl-2 genes than cisplatin, confirming that apoptosis was conspicuously promoted by 3. In addition, 3 also induced the proteolytic cleavage of PARP and obviously decreased expression level of caspase-3, while cisplatin displayed little influence on it. These results proved that the Pt(IV) conjugate 3 might possess a unique mode of action to kill cancer cells different from cisplatin owing to the conjugation with both the AR-targeting ligand and coumarin moiety.

CONCLUSIONS

Herein, we have described a type of novel AR-targeted anticancer agents produced by the conjugation of a cyanonilutamide ligand to Pt(IV) complexes derived from cisplatin and evaluated their biological activity. Electrochemical characteristics and HPLC studies revealed that the order of the chemical reduction rates of these complexes was $1 > 2 > 3$. Competitive experiments showed that all AR-Pt(IV) conjugates displayed satisfactory AR binding affinity and antagonist activity against androgen receptor. Additionally, there was greater accumulation of our complexes, especially **3**, in LNCaP (AR+) cells than in PC-3 (AR-) cells. Such differences in accumulation contributed to the selective antitumor activity in vitro. In addition, the internalization of prodrug **3** could be easily visualized by confocal microscopy due to its fluorescence property, hinting at its potential as a targeting theranostic agent. Further mechanistic research revealed that **3** arrested the cell cycle at S phase and dramatically increased the apoptosis.

Our three-in-one hybrid **3** with its innovative design is a Pt(IV) prodrug that can simultaneously bind to AR and emit fluorescence. The AR-targeted theranostic agent is able to add the AR overexpressed tumor selectivity of cisplatin and offer a promising strategy to treat CRPC.

EXPERIMENTAL SECTION

Materials and Instrument. All chemicals and solvents were of analytical reagent grade and used without further purification, unless noted specifically. c,c,t -[Pt(NH₃)₂Cl₃(OH)] and c,c,t -[Pt(NH₃)₂Cl₂(OH)₂] were prepared according to literature reports.²² The purity of all compounds used in the biological studies was $\geq 95\%$. All antibodies were purchased from Santa Cruz Biotechnology. All cancer cell lines were obtained from Jiangsu KeyGEN BioTECH company (China). Cell cycle and apoptosis experiments were measured by flow cytometry (FAC Scan, Becton Dickinson) and analyzed by Cell Quest software. ¹H NMR and ¹³C NMR spectra were recorded in DMSO-*d*₆ on a Bruker 300 MHz spectrometer. ¹⁹⁵Pt NMR spectra were measured in DMSO-*d*₆ with a Bruker 600 MHz spectrometer. Platinum contents were determined by Inductively Coupled Plasma-Mass Spectrometer (ICP-MS, Optima 5300DV, PerkinElmer, USA). Mass spectra were measured by an Agilent 6224 ESI/TOF MS instrument. Elemental analyses of C, H, and N used a Vario MICRO CHNOS elemental analyzer (Elementar).

Chemistry, Synthesis, and Characterization of 4. 4-Fluoro-2-(trifluoromethyl)benzotrile (4.02 g, 21.3 mmol) was added to a mixture of hydantoin (13.6 g, 106.3 mmol) and potassium carbonate (4.40 g, 31.9 mmol) in DMF (60 mL) and stirred at 45 °C under argon for 48 h. Reaction mixture was diluted in ethyl acetate and washed three times with water. The organic layer was dried over sodium sulfate, filtered and concentrated in vacuo. Column chromatography (eluent 30:1 DCM/Methanol) gave **6** as a white solid (4.62 g, 74%). ¹H NMR (300 MHz, DMSO-*d*₆): δ 1.42 (s, 6H), 8.01–8.04 (d, 1H), 8.18 (s, 1H), 8.29–8.32 (d, 1H), 8.84 (s, 1H) ppm.

Synthesis of 8 (L-1). Compound **6** (5.00 g, 16.8 mmol) was dissolved in DMF (40 mL) under argon, followed by addition of NaH (60% in mineral oil, 1.00 g, 25.2 mmol) and stirring for 2 h at room temperature. Then ethyl bromoacetate (4.22 g, 25.2 mmol) was added and the reaction was stirred for 5 h at 55 °C. To the reaction was added EtOAc (200 mL) and the mixture was successively washed with brine (5 \times 150 mL) and H₂O (3 \times 125 mL). The organic layer was dried over sodium sulfate, filtered and concentrated in vacuo. Column chromatography (eluent 5:1 PE/EtOAc) gave **7** as a white solid (5.21 g, 81%). Compound **7** (5.01 g, 13.1 mmol) was dissolved in MeOH (40 mL), followed by addition of NaOH (2.0 g, 50.4 mmol) and stirring for 2 h at 50 °C. The reaction mixture was concentrated, dissolved in 150 mL of H₂O and adjusted the pH value to acidity. The precipitate was filtered and dried in vacuo to get **8** as a white solid (4.55 g, 97%). ESI-HRMS: m/z [M – H][–] = 354.0699. ¹H NMR (300 MHz,

DMSO-*d*₆) δ 1.45 (s, 6H), 4.14 (s, 2H), 8.04–8.07 (d, 1H, J = 8.5 Hz), 8.20 (s, 1H), 8.30–8.33 (d, 1H, J = 8.3 Hz), 12.93 (s, 1H) ppm.

Synthesis of 11. 7-Hydroxycoumarin (1.62 g, 10 mmol), potassium carbonate (6.91 g, 50 mmol), bromoacetic acid (6.95 g, 50 mmol), and acetone (250 mL) were added into a 500 mL round-bottom flask. Then catalytic amount of potassium iodide was added. The mixture was refluxed for 20 h. The reaction was monitored by TLC. After reaction finished, water (200 mL) was added and the pH was adjusted to ~ 3 by 5% HCl aqueous. Then acetone was removed under reduced pressure at room temperature. The mixture was filtered and the solid was washed by water (30 mL \times 3) and Et₂O (30 mL \times 3). The white solid was dried, yield 89%. ¹H NMR (300 MHz, DMSO-*d*₆) δ 4.82 (s, 2H), 6.82–6.32 (d, 1H, J = 9.5 Hz), 6.94–6.97 (m, 2H), 7.62–7.65 (d, 1H, J = 9.2 Hz), 7.97–8.00 (d, 1H, J = 9.5 Hz), 13.09 (s, 1H) ppm.

Synthesis of 1. A solution of TBTU (105.6 mg, 0.33 mmol) and **8** (117.2 mg, 0.33 mmol) in 10 mL of anhydrous DMF was stirred at room temperature under N₂ atmosphere. After 10 min, TEA (33.3 mg, 0.33 mmol) was added and the reaction was stirred for 15 min, c,c,t -[Pt(NH₃)₂Cl₃(OH)] (115.8 mg, 0.33 mmol) was then added and the reaction mixture was stirred at room temperature for 12 h. The solvent was then removed by evaporation under reduced pressure. Column chromatography (eluent 15:1 DCM/methanol) gave **1** as a pale yellow solid (111.6 mg, 49%). ESI-HRMS: calcd for m/z [M – H][–], 687.9946; found, 687.9851. ¹H NMR (300 MHz, DMSO-*d*₆) δ 1.45 (s, 6H), 4.10 (s, 2H), 6.20 (m, 6H), 8.04–8.07 (d, 1H), 8.19 (s, 1H), 8.30–8.33 (d, 1H) ppm. ¹³C NMR (75 MHz, DMSO-*d*₆) δ 22.87, 42.72, 62.27, 107.38, 115.70, 121.37 (J = 274.6 Hz), 124.46 (J = 4.8 Hz), 130.44, 131.52 (J = 33.6 Hz), 136.70, 137.74, 153.23, 175.26, 175.95 ppm. ¹⁹⁵Pt NMR (129 MHz, DMSO-*d*₆) δ 552 ppm. Anal. Calcd for C₁₅H₁₇Cl₃F₃N₅O₄Pt: C, 26.12; H, 2.48; N, 10.15%. Found: C, 26.35; H, 2.59; N, 10.03%.

Synthesis of 2. A solution of TBTU (105.6 mg, 0.33 mmol) and **8** (117.2 mg, 0.33 mmol) in 40 mL of anhydrous DMF was stirred at room temperature under a N₂ atmosphere. After 10 min, TEA (33.3 mg, 0.33 mmol) was added and the reaction was stirred for 15 min, c,c,t -[Pt(NH₃)₂Cl₂(OH)₂] (110.3 mg, 0.33 mmol) was then added and the reaction mixture was stirred at 55 °C for 12 h. The solvent was then removed by evaporation under reduced pressure. Column chromatography (eluent 8:1 DCM/Methanol) gave **2** as a yellow solid (50.3 mg, 22.7%). ESI-HRMS: calcd for m/z [M – H][–], 670.0285; found, 670.0168. ¹H NMR (300 MHz, DMSO-*d*₆) δ 1.44 (s, 6H), 4.00 (s, 2H), 5.83–6.08 (m, 6H), 8.04–8.06 (d, 1H, J = 8.1 Hz), 8.19 (s, 1H), 8.31–8.33 (d, 1H, J = 8.1 Hz) ppm. ¹³C NMR (75 MHz, DMSO-*d*₆) δ 22.87, 42.78, 62.19, 107.29, 115.68, 121.35 (J = 273.3 Hz), 124.38 (J = 4.9 Hz), 130.35, 131.50 (J = 32.5 Hz), 136.66, 137.20, 153.16, 175.35, 175.95 ppm. ¹⁹⁵Pt NMR (129 MHz, DMSO-*d*₆) δ 1065 ppm. Anal. Calcd for C₁₅H₁₈Cl₂F₃N₅O₅Pt: C, 26.84; H, 2.70; N, 10.43%. Found: C, 26.65; H, 2.79; N, 10.19%.

Synthesis of 3. A solution of TBTU (35.3 mg, 0.11 mmol) and **11** (24.2 mg, 0.11 mmol) in 10 mL of anhydrous DMF was stirred at room temperature under a N₂ atmosphere. After 10 min, TEA (11.2 mg, 0.11 mmol) was added and the reaction was stirred for 15 min. Complex **2** (73.7 mg, 0.11 mmol) was then added and the reaction mixture was stirred at 25 °C for 12 h. The solvent was then removed by evaporation under reduced pressure. Column chromatography (eluent 15:1 DCM/methanol) gave **3** as a yellow solid (52.3 mg, 54.5%). ESI-HRMS: calcd for m/z [M – H][–], 872.0551; found, 872.0421. ¹H NMR (300 MHz, DMSO-*d*₆) δ 1.45 (s, 6H), 4.12 (s, 2H), 4.78 (s, 2H), 6.27–6.30 (s, 1H, J = 10.0 Hz), 6.50 (m, 6H), 6.93–6.95 (d, 1H, J = 8.7 Hz), 7.01 (s, 1H), 7.59–7.61 (d, 1H, J = 8.4 Hz), 7.97–8.00 (d, 1H, J = 9.6 Hz), 8.04–8.07 (d, 1H, J = 8.5 Hz), 8.19 (s, 1H), 8.31–8.33 (d, 1H, J = 8.4 Hz) ppm. ¹³C NMR (75 MHz, DMSO-*d*₆) δ 22.81, 41.77, 62.24, 65.01, 102.17, 107.37, 113.02, 113.05, 113.47, 115.67, 121.34 (J = 272.6 Hz), 124.42 (J = 4.6 Hz), 129.75, 130.38, 131.51 (J = 31.5 Hz), 136.69, 137.12, 144.81, 153.22, 155.74, 160.83, 161.75, 175.20, 175.27, 176.10 ppm. ¹⁹⁵Pt NMR (129 MHz, DMSO-*d*₆) δ 1231 ppm. Anal. Calcd for C₂₆H₂₄Cl₂F₃N₅O₉Pt: C, 35.75; H, 2.77; N, 8.02%. Found: C, 35.92; H, 2.90; N, 7.86%.

Cyclic Voltammetry. The cyclic voltammetry (CV) was measured on PGSTAT101 (Autolab, Metrohm) in a range of potentials from

+1.0 V to -1.0 V, with a three electrode setup comprising a glassy carbon working electrode, platinum wire auxiliary electrode and a calomel reference electrode. Complexes 1–3 were dissolved in PBS containing 5% DMF at the concentration of 20 mM. The scan rate was 100 mV·s⁻¹ at 25 °C, KCl (0.1 M, pH 7.0) was used as a background electrolyte.

Stability of Complexes 1–3 in PBS Buffer and Medium RPMI-1640. The stability of Pt(IV) complexes in a phosphate buffer saline (PBS) and RPMI-1640 supplemented with 10% fetal bovine serum was investigated by HPLC. The incubation was generated by adding different complexes into PBS buffer or RPMI-1640, which was performed at 25 °C at different times. Reversed phase HPLC was implemented on a 250 × 4.5 mm ODS column and the HPLC profiles were recorded on UV detection at 210 nm. Mobile phase consisted of acetonitrile/water, and flow rate was 1.0 mL/min. The samples were taken for HPLC analysis after filtration by 0.45 μm filter.

Reduction Ability of Pt(IV) Complexes 1–3 Treated with Ascorbic Acid. The Reduction of Pt(IV) complexes was carried out using ascorbic acid in acetonitrile/water and reduction products were examined at 25 °C by HPLC. Reversed phase HPLC was implemented on a 250 × 4.5 mm ODS column and the HPLC profiles were recorded on UV detection at 210 nm. Mobile phase consisted of acetonitrile/water (80:20, v/v), and flow rate was 1.0 mL/min. The samples were taken for HPLC analysis after filtration by 0.45 μm filter.

UV–Vis Spectral test. The UV absorption of complexes 1–3 in PBS containing 5% DMF at the concentration of 0.1 mM was recorded on a Shimadzu UV2600 instrument equipped with a thermostatically controlled cell holder. The wavelength range is 210–400 nm. All the experiments were studied at 37 ± 0.1 °C, the solvent absorption was deducted as the background.

Determination of Quantum Yields. Quantum yields were determined at 25 °C, Rhodamine B ($\Phi = 0.59$) in ethanol was used as a standard. The absorption of Rhodamine B was adjusted to the same value ($\text{abs} < 0.1$) as that of fluorescent molecules. Excitation was chosen at 320 nm; the emission spectra were corrected and integrated from 340 to 520 nm. The quantum yields were calculated with the following equation: $\Phi_{\text{sample}} = \Phi_{\text{standard}} (F_{\text{sample}}/F_{\text{standard}}) (A_{\text{sample}}/A_{\text{standard}})$. Φ is the quantum yield, F is the integration of emission intensity, and A is the absorbance value at excitation wavelength.

Preparation of Stock Solutions for Cellular Studies. Organic compounds and Pt(IV) complexes were dissolved in DMF to a final concentration of 20 mM and serially diluted prior to testing. The final DMF concentration in culture medium did not exceed 0.4%. Stock solution of cisplatin was prepared in water and diluted directly into culture medium.

Cell Culture. PC-3 (Human prostatic cancer cell line, AR-) and LNCaP (Human prostatic cancer cell line, AR+) were maintained in the logarithmic phase at 37 °C in a 5% carbon dioxide atmosphere using the following monolayer culture media containing 10% fetal bovine serum (FBS), 100 μg/mL of penicillin, and 100 μg/mL of streptomycin.

Molecular Docking Analysis. All the docking studies were carried out using Sybyl-X 2.0 on a Windows workstation. The initial coordinates for AR were taken from the crystal structure of AR in complex with testosterone (PDB: 2AM9).^{24,25} The AR-targeting ligand L-1, cyanonilutamide and the endogenous steroid testosterone were selected for the docking studies. The 3D structures of these selected compounds were first built using Sybyl-X 2.0 sketch followed by energy minimization using the MMFF94 force field and Gasteiger-Marsili charges. We employed Powell's method for optimizing the geometry with a distance dependent dielectric constant and a termination energy gradient of 0.005 kcal/mol. All the selected compounds were automatically docked into the binding pocket of AR by an empirical scoring function and a patented search engine in the Surflex docking program. Before the docking process, the natural ligand was extracted; the water molecules were removed from the crystal structure. Subsequently, the protein was prepared by using the Biopolymer module implemented in Sybyl. The polar hydrogen atoms were added. The automated docking manner was applied in the present work.

Confocal Microscopy. Cellular localization of tested compounds in LNCaP and PC-3 cells was determined by using confocal microscopy. 0.5×10^6 cells were seeded on the 35 mm glass bottom dishes

(MatTek). The cells were treated and incubated with tested compounds at 37 °C under 5% CO₂ for 4 h. Then DAPI was added during the final 15 min of the incubation. The cells were washed by phosphate buffered saline (PBS) and then imaged after further incubation in colorless serum-free media for 15 min. Fluorescence images were taken using a confocal laser scanning microscope (Zeiss LSM 700, Zeiss, Germany). Fluorescence from 11 or 3 appears as green signals (Ex: 355 nm; Em: 490–520 nm), while that from DAPI staining nucleus appears as blue signals (Ex: 340 nm; Em: 450–470 nm). Scale bar, 30 μm.

AR Ligand Binding Affinity. The fluorescence polarization technique was used to analyze the binding of L-1, 1–3, cisplatin, cyanonilutamide, and bicalutamide to the androgen receptor using the PolarScreen AR Competitor Assay, Green (lifetechnologies, A15880) according to the manufacturer's instructions. Briefly, the assay entails titration of the test compound against a preformed complex of Fluormone AL Green and the AR-LBD (GST). The assay mixture was allowed to equilibrate at room temperature in 384-well black plates for 4 h, after which the fluorescence polarization values were measured in a SpectraMax Paradigm Multi-Mode Detection Platform (Molecular Devices) using an excitation wavelength of 485 nm and an emission wavelength of 535 nm. Data analysis for the ligand binding assays was performed using Prism software (GraphPad Software, Inc.).

Luciferase Assay. Assay of androgenic activity was performed by means of ARE luciferase reporter assay using HEK 293T cells. Cells were sown in a 150 cm² flask (Corning), and cultured in culture medium (DMEM medium containing 10% Dextran Charcoal (DCC)-Fetal Bovine Serum (FBS), 2 mM glutamine) for 24 h pcDNA3.1-AR, pRLSV40, and pMMTV-Luc vector containing luciferase gene bound at the downstream of an AR promoter derived from Mouse Mammary Tumor Virus (MMTV) were cotransfected by using Lipofectamine 2000. After culturing at 37 °C in a 5% CO₂ atmosphere for 4 h, these cells were harvested and plated in a 96 well plate (10000 cells/well) and cultured for 2 h. A total of 24 h after addition of the sample (final concentration, 10 μM) and 1 nM R1881, cells were harvested with 20 μL of cell passive lysis buffer (Promega), and the firefly and Renilla luciferase activities were determined with a Dual Luciferase Assay Kit (Promega) by measuring luminescence with a Wallac Micro-Beta scintillation counter (PerkinElmer Life Sciences). The data were obtained in triplicate and expressed as inhibition rate over the R1881 control. $\text{Inhibition\%} = 1 - (\text{RLU}_{\text{test}} - \text{RLU}_{\text{blank}}) / (\text{RLU}_{\text{R1881}} - \text{RLU}_{\text{blank}}) \times 100\%$. RLU = relative light unit.

Cytotoxicity Measurement. The in vitro activity of the synthesized compounds was determined by the MTT method. The cultured cells with better vitality were transferred to a 96-well plate so that the density of the cells was 5000 per well, and they were incubated overnight. Then, the compounds were dissolved in DMF and diluted with medium to various concentrations (the final concentration of DMF was less than 0.4%). After being incubated at 37 °C for 72 h, cells were stained with 3-(4,5-dimethyl-2-thiazolyl)-2,5-diphenyl-2H-tetrazolium bromide (MTT; 5 mg/mL) for another 4 h, and then dissolved with 150 μL of DMSO. The UV absorption intensity was detected with an ELISA reader at 490 nm. The IC₅₀ values were calculated by SPSS software after three parallel experiments.

Cellular Uptake Test. LNCaP and PC-3 cells with good activity were seeded in 6-well plates at 37 °C in 5% CO₂. After the cell density reached 80%, cisplatin or complexes 1–3 was added to each well at a concentration of 20 μM, and the plates were incubated for 12 h. Then, cells were collected and washed three times with ice-cold PBS, followed by centrifugation for 10 min and resuspension in PBS (1 mL). Then, 100 μL of suspension was taken out for measuring the cell density. The remaining cells were digested by HNO₃ (200 μL, 65%) at 65 °C for 10 min. The results were measured by ICP-MS after three parallel experiments.

Apoptosis Analysis. LNCaP cells were used in the apoptosis experiment. Cisplatin was the positive control at a concentration of 20 μM. Specific operations were as follows: LNCaP cells with good activity (5×10^5 cells per plate) were transferred to six-well plates and cultured overnight in 5% CO₂ at 37 °C. Drugs were added, which were diluted to a concentration of 20 μM. After 24 h, the cells were digested

with trypsin and washed twice with cold PBS. Then, cells were collected by centrifugation (2000 rpm, 5 min). After that, cells were resuspended in binding buffer (10 mM HEPES, 140 mM NaCl, 2.5 mM CaCl₂, pH 7.4) and incubated with annexin V-VAPC (100 ng/mL) and then with propidium iodide (2 μg/mL) for 15 min in the dark at room temperature. At last, the fluorescence of cells was detected by an annexin V-APC/7-AAD apoptosis detection kit (Roche) according to the manufacturer's protocol, and cells were analyzed by a computer station running Cell Quest software.

Cell Cycle Measurement. LNCaP cells with good vitality were transferred into six-well plates, with a density of 10000 per well, and cultured overnight at 37 °C. Then, 20 μM of the tested compounds were incubated with cells for 24 h. All adherent and floating cells were collected and washed twice with PBS. Then, the cells were fixed with 70% EtOH at 4 °C for 24 h. After that, fixed cells were washed with PBS. After being centrifuged, cells were stained with 50 μg/mL propidium iodide solution containing 100 μg/mL RNase at 37 °C for 0.5 h. The sample (at least 1 × 10⁴ cells) was measured by flow cytometry (FAC Scan, Becton Dickinson) using Cell Quest software and recording propidium iodide (PI) in the FL2 channel.

Western Blot. The active preferred LNCaP cells were seeded until the cell density reached 80%. Then 20 μM of the compounds were added, and the cells were cultured for 12 h at 37 °C. Proteins were extracted by lysis buffer. The concentration of protein was measured by the BCA (bicinchoninic acid) assay with a Varioskan multimode microplate spectrophotometer (Thermo, Waltham, MA). Then equal amounts of protein (20 mg/Lane) were separated by 10% sodium dodecyl sulfate-polyacrylamide gel electrophoresis (SDS-PAGE). After that, protein samples were transferred onto polyvinylidene difluoride (PVDF) Immobilon-P membrane (Bio-Rad) with a transblot apparatus (Bio-Rad). The blots, blocked with 5% nonfat milk in TBST (Tris-buffered saline plus 0.1% Tween 20) for 1 h, were incubated with primary antibodies diluted in PBST overnight at 4 °C. After that, the membrane was washed with PBST three times and incubated with IRDye 800 conjugated secondary antibody for 1 h at 37 °C. Detection was performed by an Odyssey scanning system (Li-COR, Lincoln, Nebraska).

■ ASSOCIATED CONTENT

● Supporting Information

The Supporting Information is available free of charge on the ACS Publications website at DOI: 10.1021/acs.inorgchem.8b00083.

Diagrams of ESI-MS, ¹H, ¹³C and ¹⁹⁵Pt NMR spectra. Cyclic voltammograms of complexes 1–3. HPLC analyses on the stability and the released ability of Pt(IV) complexes under reduction with ascorbic acid (PDF).

■ AUTHOR INFORMATION

Corresponding Author

*E-mail: sgou@seu.edu.cn.

ORCID

Shaohua Gou: 0000-0003-0284-5480

Author Contributions

[§]These authors contributed equally to this work.

Notes

The authors declare no competing financial interest.

■ ACKNOWLEDGMENTS

The authors are grateful to the National Natural Science Foundation of China (Grant Nos. 21571033 and 21601034) for financial aid to this work. We also want to thank Fundamental Research Funds for the Central Universities (Project 2242016K30020) and Priority Academic Program Development of Jiangsu Higher Education Institutions for the construction of fundamental facilities. Jiangsu KeyGen Biotech Company is appreciated for

completing the AR binding affinity and antagonist activity studies. We would like to express our gratitude to Prof. Hengshan Wang (Guangxi Normal University) for a license to use their software. We would like to thank LetPub (www.letpub.com) for providing linguistic assistance during the preparation of this manuscript.

■ ABBREVIATIONS

DMSO dimethyl sulfoxide; DCM dichloromethane; TEA triethylamine; DMF *N,N'*-dimethylformamide; PBS phosphate buffer solution; TBTU *O*-(benzotriazol-1-yl)-*N,N,N',N'*-tetramethyluronium tetrafluoroborate; ICP-MS inductively coupled plasma mass spectrometry; VC ascorbic acid; CV cyclic voltammetry; AR androgen receptor

■ REFERENCES

- (1) Jemal, A.; Siegel, R.; Ward, E.; Hao, Y.; Xu, J.; Thun, M. J. CA: a cancer journal for clinicians. *Ca-Cancer J. Clin.* **2009**, *59*, 225–249.
- (2) Torre, L. A.; Bray, F.; Siegel, R. L.; Ferlay, J.; Lortet-tieulent, J.; Jemal, A. Global cancer statistics. *Ca-Cancer J. Clin.* **2015**, *65* (2), 87–108.
- (3) Delaere, K. P.; Van Thillo, E. L. Flutamide monotherapy as primary treatment in advanced prostatic carcinoma. *Semin. Oncol.* **1991**, *18*, 13–18.
- (4) Kolvenbag, G. J.; Blackledge, G. R.; Gotting-Smith, K. Bicalutamide (Casodex®) in the treatment of prostate cancer: history of clinical development. *Prostate* **1998**, *34*, 61–72.
- (5) Ferroni, C.; Pepe, A.; Kim, Y. S.; Lee, S.; Guerrini, A.; Parenti, M. D.; De Cesare, M. 1, 4-substituted triazoles as nonsteroidal anti-androgens for prostate cancer treatment. *J. Med. Chem.* **2017**, *60*, 3082–3093.
- (6) Oudard, S. Progress in emerging therapies for advanced prostate cancer. *Cancer Treat. Rev.* **2013**, *39*, 275–289.
- (7) (a) Clegg, N. J.; Wongvipat, J.; Joseph, J. D.; Tran, C.; Ouk, S.; Dilhas, A.; Chen, Y.; Grillot, K.; Bischoff, E. D.; Cai, L.; Aparicio, A. ARN-509: a novel antiandrogen for prostate cancer treatment. *Cancer Res.* **2012**, *72*, 1494–1503. (b) Lin, H. M.; Mahon, K. L.; Weir, J. M.; Mundra, P. A.; Spleman, C.; Briscoe, K.; Gurney, H.; Mallesara, G.; Marx, G.; Stockler, M. R.; Consortium, P.; Parton, R. G.; Hoy, A. J.; Daly, R. J.; Melkel, P. J.; Horvath, L. G. A distinct plasma lipid signature associated with poor prognosis in castration-resistant prostate cancer. *Int. J. Cancer* **2017**, *141*, 2112–2120. (c) Beer, T. M.; Hotte, S. J.; Saad, F.; Alekseev, B.; Matveev, V.; Fléchon, A.; Gravis, G.; Joly, F.; Chi, K. N.; Malik, Z.; Blumenstein, B. Custirsens (OGX-011) combined with cabazitaxel and prednisone versus cabazitaxel and prednisone alone in patients with metastatic castration-resistant prostate cancer previously treated with docetaxel (AFFINITY): a randomised, open-label, international, phase 3 trial. *Lancet Oncol.* **2017**, *18*, 1532–1542.
- (8) Balk, S. P. Androgen receptor as a target in androgen-independent prostate cancer. *Urology* **2002**, *60*, 132–138.
- (9) Mohler, J. L.; Gregory, C. W.; Ford, O. H., III; Kim, D.; Weaver, C. M.; Petrusz, P.; Wilson, E. M.; French, F. S. The androgen axis in recurrent prostate cancer. *Clin. Cancer Res.* **2004**, *10*, 440–448.
- (10) Culig, Z.; Klocker, H.; Bartsch, G.; Hobisch, A. Androgen receptors in prostate cancer. *Endocr.-Relat. Cancer* **2002**, *9*, 155–170.
- (11) Gustafson, J. L.; Neklesa, T. K.; Cox, C. S.; Roth, A. G.; Buckley, D. L.; Tae, H. S.; Sundberg, T. B.; Blake Stagg, D.; Hines, J.; McDonnell, D. P.; Norris, J. D.; Crews, C. M. Small-molecule-mediated degradation of the androgen receptor through hydrophobic tagging. *Angew. Chem.* **2015**, *127*, 9795–9798.
- (12) Linja, M. J.; Savinainen, K. J.; Saramaki, O. R.; Tammela, T. L. J.; Vessella, R. L.; Visakorpi, T. Amplification and overexpression of androgen receptor gene in hormone-refractory prostate cancer. *Cancer Res.* **2001**, *61*, 3550–3555.
- (13) Marom, H.; Miller, K.; Bechor-Bar, Y.; Tsarfaty, G.; Satchi-Fainaro, R.; Gozin, M. Toward development of targeted nonsteroidal

antiandrogen-1, 4, 7, 10-tetraazacyclododecane-1, 4, 7, 10-tetraacetic acid-gadolinium complex for prostate cancer diagnostics. *J. Med. Chem.* **2010**, *53*, 6316–6325.

(14) Cogan, P. S.; Koch, T. H. Rational design and synthesis of androgen receptor-targeted nonsteroidal anti-androgen ligands for the tumor-specific delivery of a doxorubicin-formaldehyde conjugate. *J. Med. Chem.* **2003**, *46*, 5258–5270.

(15) Gryder, B. E.; Akbashev, M. J.; Rood, M. K.; Rafferty, E. D.; Meyers, W. M.; Dillard, P.; Oyelere, A. K. Selectively targeting prostate cancer with antiandrogen equipped histone deacetylase inhibitors. *ACS Chem. Biol.* **2013**, *8*, 2550–2560.

(16) Scher, H. I.; Beer, T. M.; Higano, C. S.; Anand, A.; Taplin, M. E.; Efstathiou, E.; Rathkopf, D.; Shelkey, J.; Yu, E. Y.; Alumkal, J. Antitumor activity of MDV3100 in castration-resistant prostate cancer: a phase 1–2 study. *Lancet* **2010**, *375*, 1437–1446.

(17) Rapozzi, V.; Ragno, D.; Guerrini, A.; Ferroni, C.; Pietra, E. D.; Cesselli, D.; Varchi, G. Androgen receptor targeted conjugate for bimodal photodynamic therapy of prostate cancer in vitro. *Bioconjugate Chem.* **2015**, *26*, 1662–1671.

(18) Abu-Surrah, A. S.; Kettunen, M. Platinum group antitumor chemistry: design and development of new anticancer drugs complementary to cisplatin. *Curr. Med. Chem.* **2006**, *13*, 1337–1357.

(19) Wheate, N. J.; Walker, S.; Craig, G. E.; Oun, R. The status of platinum anticancer drugs in the clinic and in clinical trials. *Dalton Trans.* **2010**, *39*, 8113–8127.

(20) Galanski, M.; Jakupec, M. A.; Keppler, B. K. Update of the preclinical situation of anticancer platinum complexes: novel design strategies and innovative analytical approaches. *Curr. Med. Chem.* **2005**, *12*, 2075–2094.

(21) Zheng, Y. R.; Suntharalingam, K.; Johnstone, T. C.; Lippard, S. J. Encapsulation of Pt(IV) prodrugs within a Pt(II) cage for drug delivery. *Chem. Sci.* **2015**, *6*, 1189–1193.

(22) Huxley, M.; Sanchez-Cano, C.; Browning, M. J.; Navarro-Ranninger, C.; Quiroga, A. G.; Rodger, A.; Hannon, M. J. An androgenic steroid delivery vector that imparts activity to a non-conventional platinum(II) metallo-drug. *Dalton Trans.* **2010**, *39*, 11353–11364.

(23) (a) Wang, Z.; Xu, Z.; Zhu, G. A platinum(IV) anticancer prodrug targeting nucleotide excision repair to overcome cisplatin resistance. *Angew. Chem., Int. Ed.* **2016**, *55*, 15564–15568. (b) Ma, L.; Ma, R.; Wang, Y.; Zhu, X.; Zhang, J.; Chan, H.; Chen, X.; Zhang, W.; Chiu, S.; Zhu, G. Chalcoplatin, a dual-targeting and p53 activator-containing anticancer platinum(IV) prodrug with unique mode of action. *Chem. Commun.* **2015**, *51*, 6301–6304.

(24) Xu, Z. C.; Zhao, J.; Gou, S. H.; Xu, G. Novel hypoxia-targeting Pt(IV) prodrugs. *Chem. Commun.* **2017**, *53*, 3749–3752.

(25) (a) Pathak, R. K.; Marrache, S.; Choi, J. H.; Berding, T. B.; Dhar, S. The prodrug platin-A: simultaneous release of cisplatin and aspirin. *Angew. Chem., Int. Ed.* **2014**, *53*, 1963–1967. (b) Wong, D. Y. Q.; Yeo, C. H. F.; Ang, W. H. Immuno-chemotherapeutic platinum(IV) prodrugs of cisplatin as multimodal anticancer agents. *Angew. Chem., Int. Ed.* **2014**, *53*, 6752–6756.

(26) Dhar, S.; Gu, F. X.; Langer, R.; Farokhzad, O. C.; Lippard, S. J. Targeted delivery of cisplatin to prostate cancer cells by aptamer functionalized Pt(IV) prodrug-PLGA-PEG nanoparticles. *Proc. Natl. Acad. Sci. U. S. A.* **2008**, *105*, 17356–17361.

(27) Barnes, K. R.; Kutikov, A.; Lippard, S. J. Synthesis, characterization, and cytotoxicity of a series of estrogen-tethered platinum(IV) complexes. *Chem. Biol.* **2004**, *11*, 557–564.

(28) Dreaden, E. C.; Gryder, B. E.; Austin, L. A. Antiandrogen gold nanoparticles dual-target and overcome treatment resistance in hormone-insensitive prostate cancer cells. *Bioconjugate Chem.* **2012**, *23*, 1507–1512.

(29) Rehan, M.; Ahmad, E.; Sheikh, I. A.; Abuzenadah, A. M.; Damanhour, G. A.; Bajouh, O. S.; Al Basri, S. F.; Assiri, M. M.; Beg, M. A. Androgen and progesterone receptors are targets for bisphenol A (BPA), 4-methyl-2, 4-bis-(p-hydroxyphenyl)pent-1-ene-a potent metabolite of BPA, and 4-tert-octylphenol: a computational insight. *PLoS One* **2015**, *10*, e0138438/1–e0138438/18.

(30) Guo, C.; Linton, A.; Kephart, S.; Ornelas, M.; Pairish, M.; Gonzalez, J.; Greasley, S.; Nagata, A.; Burke, B. J.; Edwards, M.; Hosea, N.; Kang, P.; Hu, W.; Engebretsen, J.; Briere, D.; Shi, M.; Gukasyan, H.; Richardson, P.; Dack, K.; Underwood, T.; Johnson, P.; Morell, A.; Felstead, R.; Kuruma, H.; Matsimoto, H.; Zoubeydi, A.; Gleave, M.; Los, G.; Fanjul, A. N. Discovery of aryloxy tetramethylcyclobutanes as novel androgen receptor antagonists. *J. Med. Chem.* **2011**, *54*, 7693–7704.

(31) Lemma, K.; Sargeson, A. M.; Elding, L. I. Kinetics and mechanism for reduction of oral anticancer platinum(IV) dicarboxylate compounds by L-ascorbate ions. *J. Chem. Soc., Dalton Trans.* **2000**, *7*, 1167–1172.

(32) Choi, S.; Filotto, C.; Bisanzo, M.; Delaney, S.; Lagasee, D.; Whitworth, J. L.; Jusko, A.; Li, C.; Wood, N. A.; Willingham, J.; Schwenker, A.; Spaulding, K. Reduction and anticancer activity of platinum(IV) complexes. *Inorg. Chem.* **1998**, *37*, 2500–2504.

(33) Lemma, K.; Berglund, J.; Farrell, N.; Elding, L. I. Kinetics and mechanism for reduction of anticancer-active tetrachloroam(m)ine platinum(IV) compounds by glutathione. *JBIC, J. Biol. Inorg. Chem.* **2000**, *5*, 300–306.

(34) Zhang, J. Z.; Wexselblatt, E.; Hambley, T. W.; Gibson, D. Pt(IV) analogs of oxaliplatin that do not follow the expected correlation between electrochemical reduction potential and rate of reduction by ascorbate. *Chem. Commun.* **2012**, *48*, 847–849.